



Cite this: *Nanoscale*, 2016, **8**, 5852

Received 30th October 2015,
 Accepted 21st February 2016

DOI: 10.1039/c5nr07587d

www.rsc.org/nanoscale

Polymeric near-infrared absorbing dendritic nanogels for efficient *in vivo* photothermal cancer therapy†

Maria Molina, Stefanie Wedepohl and Marcelo Calderón*

In recent years, several near-infrared light absorbing inorganic nanomaterials have been developed for photothermal therapy. However, their biological fate after injection limits their clinical utilization. In this work, we developed a novel polymeric near-infrared light absorbing material based on a biocompatible thermoresponsive nanogel that is semi-interpenetrated with polyaniline, a conjugated polymer with strong near-infrared absorbance. This polymeric nanocomposite generates heat after being irradiated by NIR light, thereby inducing a local hyperthermia that is used for photothermal cancer therapy *in vitro* and *in vivo*.

Introduction

Photothermal therapy (PTT) has emerged as promising anti-cancer therapy due to its high specificity and efficacy. PTT is based on the conversion of light into heat to generate a mild or severe local hyperthermia which leads to different results like cell sensitization or ablation, enhanced tissue penetration by temperature-induced increase in the tissue pore size, and drug triggered release.¹ Near-infrared (NIR) light has the key advantage of being minimally absorbed by skin and tissues. Within the NIR window, which comprises wavelengths of about 650 to 900 nm, light can penetrate tissue in the order of hundreds of micrometers to centimeters. In the last decade, different inorganic materials with photothermal properties have been used successfully in anticancer therapy.² Photoactive materials such as carbon nanotubes,³ magnetic nanomaterials,⁴ or gold nanoparticles,⁵ activated with NIR radiation, were shown to be effective in the hyperthermic treatment of different cancers.⁶ However, there are still some issues related to biocompatibility and biodegradability of those inorganic nanomaterials that limit their applicability.⁷ As an

approach to solve this problem, conjugated polymers have been studied as photothermal agents in the last few years. NIR absorbing, conjugated polymers show excellent photostability, good biocompatibility, and high photothermal conversion.^{8–10} Because their major drawback is the low solubility in water, different strategies have been followed to increase their solubility, whereby stabilization of the conjugated polymeric nanoparticles with water-soluble polymers has been the most studied one.¹¹ Until now, semi-interpenetration (SIPN) within hydrophilic nanosized networks has not been considered.

In order to create well-defined, monodisperse, and stable nanostructures on the molecular level, highly branched dendritic polymers have been successfully employed over the last couple of decades. There has been much interest in the fabrication of dendritic nanogels (NGs), which are high molecular weight crosslinked polymers that combine the characteristics of dendritic polymers with crosslinked macroscopic gels to yield soluble particles with a useful size range between 20 and 200 nm.¹² Temperature-sensitive NG systems are versatile in design, their phase transition temperatures can be tuned, and they feature passive targeting ability.¹³ By combining thermoresponsive polymers with dendritic polyglycerol (dPG), our group has developed a series of dendritic thermoresponsive NGs that are suitable for biomedical applications.^{14–16} The presence of dPG as a macro-crosslinker, attached *via* a biodegradable ester linkage, provides high biocompatibility and hydrophilicity and, more importantly, can avoid the precipitation of the NGs in the collapse state above the transition temperature (T_p). In an effort to further control the existing temperature-responsive systems, current studies have combined temperature with other stimuli such as pH and light.¹⁷ NIR absorbers have been combined with thermoresponsive gels in order to use NIR light as an external trigger for structural changes in thermoresponsive materials.^{18,19}

Herein, we have synthesized a thermoresponsive poly(*N*-isopropylacrylamide) (PNIPAM) based NG crosslinked with dPG and semi-interpenetrated with polyaniline (PANI) which generates heat after being irradiated by NIR light, thereby inducing a local hyperthermia (Fig. 1) for its use in PTT. At the body

Institute of Chemistry and Biochemistry, Freie Universität Berlin, Takustrasse 3, 14195 Berlin, Germany. E-mail: marcelo.calderon@fu-berlin.de;
<http://www.bcp.fu-berlin.de/chemie/calderon>; Fax: (+)49-030-838459368

† Electronic supplementary information (ESI) available. See DOI: 10.1039/c5nr07587d



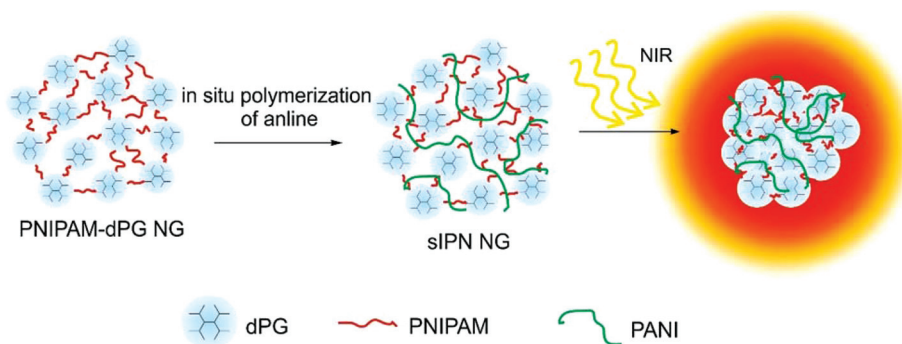


Fig. 1 Schematic representation of the synthesis of a semi-interpenetrating NIR-thermosensitive NG and its application in PTT.

temperature, the shape of the dendritic NG changes because of its thermoresponsive properties, which triggers its shrinkage, but, due to the presence of dPG, the collapsed NG still has good suspension and does not precipitate. In this hydrophobic state, as observed in previous reports, the collapsed NGs can be expected to more easily accumulate in cells and/or penetrate tissues.²⁰

Results and discussion

NGs based on PNIPAM crosslinked with 33 wt% of dPG (PNIPAM-dPG) were synthesized following the procedure previously reported by our group.¹⁴ In a further step, PNIPAM-dPG/PANI NGs were synthesized following a two-step semi-interpenetration procedure. Briefly, dry NGs were swollen in a solution of aniline and polymerization was started *in situ* by the addition of ammonium persulfate. To establish the conditions for the *in situ* polymerization of PANI inside the NGs to form a nanocomposite, different reaction conditions were screened (Table 1).

At low concentrations of aniline (0.05 M) or short polymerization times (7 min), oligomers of aniline were obtained. When a high concentration of aniline was used, the PANI started to precipitate out of the solution. Using 0.1 M of aniline and 30 min of polymerization time, a stable PANI dispersion with a reproducible size and thermoresponsive properties was obtained (PNIPAM-dPG/PANI).

The *in situ* polymerization of aniline was confirmed by ¹H-NMR, FTIR, and UV-Vis measurements (ESI[†]). After the semi-interpenetration of the NIR absorbing polymer into the NGs, two new bands corresponding to the PANI appeared in the FTIR spectrum with the C=C stretching at 1590 cm⁻¹ and the C-N stretching absorption band at 1310 cm⁻¹, while all the absorption bands of the PNIPAM and dPG remained the same.¹⁴ Moreover, the ¹H-NMR spectrum confirmed the presence of PANI in the composite with a peak at ~7.4 ppm corresponding to the aromatic protons. On the other hand, after the *in situ* polymerization of aniline inside the NG, a typical UV-Vis spectrum of PANI was observed. The spectra changed with the pH in accordance with those previously reported for PANI films in the emeraldine state.²¹ This result indicates that the PANI chains inserted into the NG were unaltered and responsive to changes in the solution environment.

Atomic force microscopy (AFM) and cryogenic transmission electronic microscopy (cryoTEM) showed spherical individual nanoparticles and some aggregates. In the AFM micrographs (Fig. 2A) we observed that the NGs appear like core-shell structures. This could be explained by the synthetic procedure in agreement with the results shown by Zhang *et al.*²² At the beginning of the reaction, due to the interaction of aniline

Table 1 Reaction conditions for sIPN NG synthesis

NG (mg mL ⁻¹)	Aniline (M)	Polymerization time (min)	Results
10	0.05	30	Oligomers
10	0.1	30	PANI dispersion
10	0.1	7	Not reproducible
10	0.5	30	PANI precipitate

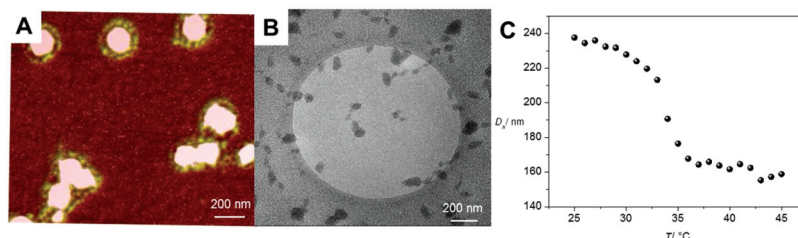


Fig. 2 Characterization of PNIPAM-dPG/PANI NGs. (a) AFM, (b) cryoTEM, and (c) hydrodynamic diameter (D_h) vs. temperature (T) as measured by DLS.



with PNIPAM, the concentration of aniline inside the NG was much higher and the polymerization started inside the network. After that, the reaction mainly took place on the surface of the NG. Thus, the particles underwent structural changes from PNIPAM-dPG to sIPN and finally to the sIPN-PANI core-shell throughout the reaction.

Dynamic light scattering (DLS) measurements revealed an increment of 100 nm in the size of the bare NGs after the semi-interpenetration, while the T_p remained the same (~ 34 °C) (Fig. 2C). Above the T_p , the size of the composites decreased from 220 nm to 150 nm. To further prove the colloidal stability of the NGs above the T_p , nanoparticle tracking analysis (NTA) was performed, which made it possible to count the particles at different temperatures. In the case of the PNIPAM-dPG/PANI NGs, the concentration of the particles was constant, $\sim 1.2 \times 10^9$ particles per mL at 25 and 42 °C, which demonstrated that the NGs had neither aggregated nor precipitated. Moreover the amount of the incorporated PANI was studied by UV-Vis and was found to be 0.9 mg of PANI per mg of PNIPAM-dPG.

As the material was supposed to be applied in PTT, we studied the increase in the temperature of the nanocomposites under NIR irradiation. Fig. 3 shows how the increase in temperature depended on the concentration of the nanocomposite and irradiation time. When only water was irradiated, the temperature increased by a maximum of 3 °C while with $20 \mu\text{g mL}^{-1}$ of nanocomposites, the temperature increased by 8 °C after 10 min of irradiation, which is enough for mild hyperthermia conditions.²³

After studying the outstanding physicochemical properties of the sIPN NGs, further biological characterization was performed in order to use these systems *in vivo*. The cytotoxicity of PNIPAM and PNIPAM-dPG/PANI on A2780 human ovarian carcinoma cells was determined by the MTT assay. The A2780 cells that had been incubated for 48 hours with PNIPAM-dPG or PNIPAM-dPG/PANI showed no reduction in viability up to

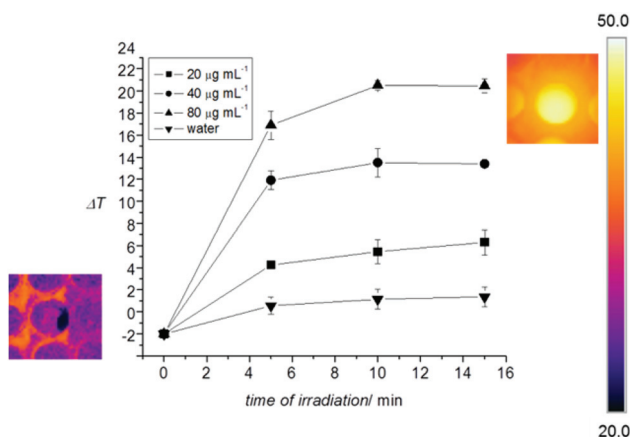


Fig. 3 Change in temperature vs. time of irradiation for dispersions of PNIPAM-dPG/PANI at different concentrations. Thermographic images on the left and right show the well in which the test with a solution of $80 \mu\text{g mL}^{-1}$ of PNIPAM-dPG/PANI was performed (scale on the right: false color code).

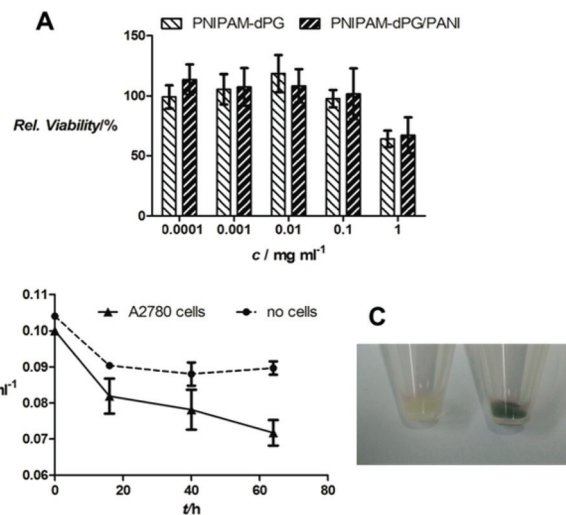


Fig. 4 (a) Cytotoxicity of PNIPAM and PNIPAM-dPG/PANI on A2780 cells as determined by the MTT assay. (b) PNIPAM-dPG/PANI concentration in culture medium of A2780 cells as determined by absorbance measurements over time. (c) Color of the cell pellet after incubation with PNIPAM-dPG/PANI (right) compared to untreated cells (left).

0.1 mg mL^{-1} and relative viabilities over 50% at a concentration of 1 mg mL^{-1} (Fig. 4a). The uptake of PNIPAM-dPG/PANI into cells was indirectly monitored by determining the concentration in the cell culture supernatant (Fig. 4b). After 64 h, the concentration was about $30 \mu\text{g mL}^{-1}$ less than that initially incubated. In addition, we observed that the cells were dark colored after trypsinization and washing with phosphate buffered saline (PBS) or media (Fig. 4c). The color remained after repeated trypsinization, reculturing, and washing which confirmed that the compound was located inside the cells.

For the study of the photothermal effect *in vitro*, the cells were released from the cell culture flask, washed, and centrifuged into PCR tubes that allowed a rapid transmission of heat through the walls of the tubes. After removing most of the media, the pellet of 1 million cells had about the volume of a

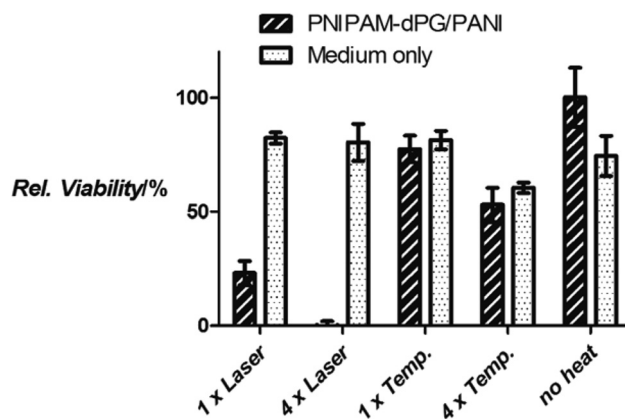


Fig. 5 Relative viabilities of A2780 cells treated with PNIPAM-dPG/PANI or untreated, irradiated with NIR laser or heated to 42 °C ("Temp.").



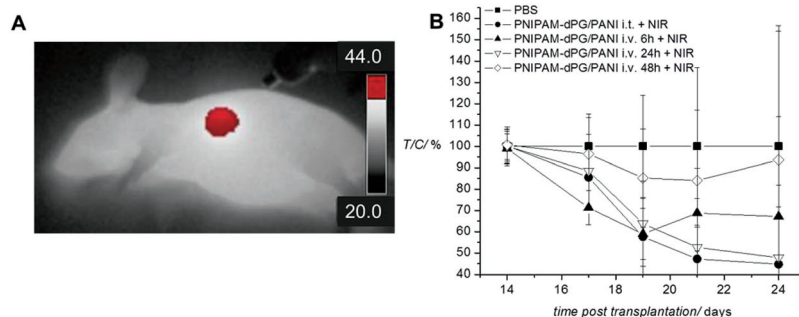


Fig. 6 (a) Thermographic image of a mouse injected with PNIPAM-dPG/PANI after 10 min irradiation and (b) tumor volume change [treated to control (T/C)] (%) of tumors in female nude mice treated at day 14 after transplantation with PBS, PNIPAM-dPG, PNIPAM-dPG/PANI, with and without irradiation.

5 μL drop, which resembled a small tumor tissue. This cluster was irradiated with a NIR laser (785 nm) under constant monitoring with a thermal camera to ensure that the temperature did not exceed $42\text{ }^{\circ}\text{C} \pm 1\text{ }^{\circ}\text{C}$. As control for the effect of hyperthermia alone, parallel samples were incubated in a water bath at $42\text{ }^{\circ}\text{C}$. Irradiation or heating was performed either one time for 5 min or four times for 5 min each with the PNIPAM-dPG/PANI incubated cells as well as untreated cells. The viabilities were measured by the MTT assay 24 h after re-seeding the treated cells into 96-well plates (Fig. 5). The A2780 cells which had taken up PNIPAM-dPG/PANI irradiated with a NIR laser showed a markedly reduced viability after a single treatment for 5 min, compared to 80% of the untreated control cells that had been irradiated for the same time. Moreover, 4 irradiation cycles resulted in a complete loss of the cell viability, whereas the control cells again were not compromised. The effect of hyperthermia for 5 min alone was not different from the controls; we only saw a decrease in viability to about 60% when the hyperthermia was repeated 4 times. As a control for the stress from centrifuging and standing as a cell cluster for a prolonged period of time outside of the incubator, another cell sample was treated under the same conditions but neither heated nor irradiated. The viability of these control cells was not markedly affected and was comparable to the untreated cells in the other series (Fig. 5, columns labeled “no heat”). This result demonstrated the efficacy of the focus heat generation compared to the whole-body hyperthermia.

This promising result encouraged us to further use these systems for localized hyperthermia therapy. Therefore the *in vivo* tolerability of the PNIPAM-dPG/PANI NGs was studied in female nude (NMRI, nu/nu) mice in a two-step protocol. The mice were first treated with a single injection of increasing doses of PNIPAM-dPG/PANI from 10 to 100 mg kg^{-1} and the body weight was measured for a period of 3 weeks. The results showed that the mice tolerated up to 100 mg kg^{-1} without any significant signs of toxicity or drug related body weight loss when given intravenously as a single dose (ESI†). Next, 3 mice were treated with the maximum injected dose, 100 mg kg^{-1} once per day during 5 consecutive days. The mice were observed for a follow-up period of 18 days. The treatment

resulted in blue-stained ear ends and tails, but the color washed out within two days. No significant toxic effects were observed during this period (accumulated dose: 500 mg kg^{-1}) (ESI†).

Once the high *in vivo* tolerability of this encouraging material was proved, we proceeded to study the therapeutic effect *in vivo*. A2780 tumor transplants were obtained from tumors, cut into small pieces and transplanted subcutaneously into female nude mice (Taconic). The mean tumor volume at this time was $0.086\text{--}0.088\text{ cm}^3$. The mice were injected intratumorally or intravenously with a single dose of 10 or 100 mg kg^{-1} of PNIPAM-dPG/PANI, respectively, or PBS and PNIPAM-dPG as controls. At the indicated time points, the mice were narcotized and the tumors were exposed to NIR laser light at a distance of about 5 cm for 5 min at a maximum radiation power of 500 mW. The tumor volume and body weight were then monitored two to three times a week until day 39. Fig. 6 summarizes the tumor volume change [treated to control (T/C)] resulting from the different treatments.

There was no or only a weak inhibitory effect of the NGs without NIR irradiation as well as with the control PNIPAM-dPG with irradiation. In contrast, intratumoral injection of PNIPAM-dPG/PANI followed by NIR treatment resulted in a tumor growth inhibition by 55.3%. When injected intravenously, the therapeutic effect was expected to depend on the successful accumulation of the particles in the tumor region in sufficient concentrations. The NGs were injected intravenously and the tumor was irradiated after 6, 24, or 48 h. When NIR treatment was done after 6 h, tumor growth inhibition was about 30%, and after 48 h, only $\sim 8\%$. Tumor growth inhibition was optimal when irradiating 24 h after intravenous injection, resulting in a tumor growth inhibition of $\sim 52.2\%$, which was nearly as effective as intratumoral injection. Our results indicated that the passive accumulation of the NGs in the tumor was sufficiently concentrated to allow a successful treatment.

Conclusions

In summary, we have formulated NIR light sensitive organic nanoparticles based on PNIPAM-dPG/PANI as a novel photo-



thermal agent and used for highly effective *in vivo* hyperthermia treatment of cancer cells. By semi-interpenetrating conjugated polymers in thermoresponsive polymeric NGs, a nanocomposite was obtained with excellent compatibility in physiological environments. This platform provides an opportunity to load the NG with anticancer drugs as well as to attach targeting moieties to the dPG. Thus, these nanoparticles appear promising for cancer therapy. Moreover, the studies *in vivo* showed that the mice tolerated up to 100 mg kg⁻¹ of PNIPAM-dPG/PANI, given at 5 consecutive days (accumulated dose: 500 mg kg⁻¹) without any significant sign of toxicity. Furthermore, the therapeutic effect study indicated that the combination of systemic treatment with PNIPAM-dPG/PANI and NIR exposure resulted in a higher sensitivity of the tumors compared to the controls alone or with NIR. Based on the simplicity and the low cost of synthesis together with the low cytotoxicity, high tolerability, and promising therapeutic effect *in vivo*, PNIPAM-dPG/PANI has been shown to be an excellent candidate for further studies. This work shows the first approach to use PNIPAM-dPG/PANI in PTT; additional strategies to enhance targeting and synergetic PTT combined with chemotherapy are currently being investigated by our group.

Acknowledgements

We gratefully acknowledge financial support from the Bundesministerium für Bildung und Forschung (BMBF) through the NanoMatFutur award (13N12561). M. Molina acknowledges financial support from the Alexander von Humboldt foundation. We gratefully thank Dr P. Winchester for proofreading the manuscript and Dr Böttcher for cryo-TEM measurements.

References

- 1 K. F. Chu and D. E. Dupuy, *Nat. Rev. Cancer*, 2014, **14**, 199–208.
- 2 D. Jaque, L. Martinez Maestro, B. del Rosal, P. Haro-Gonzalez, A. Benayas, J. L. Plaza, E. Martin Rodriguez and J. Garcia Sole, *Nanoscale*, 2014, **6**, 9494–9530.
- 3 R. Singh and S. V. Torti, *Adv. Drug Delivery Rev.*, 2013, **65**, 2045–2060.
- 4 C. S. Kumar and F. Mohammad, *Adv. Drug Delivery Rev.*, 2011, **63**, 789–808.
- 5 W.-S. Kuo, C.-N. Chang, Y.-T. Chang, M.-H. Yang, Y.-H. Chien, S.-J. Chen and C.-S. Yeh, *Angew. Chem., Int. Ed.*, 2010, **49**, 2711–2715.
- 6 L. Cheng, C. Wang, L. Feng, K. Yang and Z. Liu, *Chem. Rev.*, 2014, **114**, 10869–10939.
- 7 M. Molina, M. Asadian-Birjand, J. Balach, J. Bergueiro, E. Miceli and M. Calderon, *Chem. Soc. Rev.*, 2015, **44**, 6161–6186.
- 8 L. Xu, L. Cheng, C. Wang, R. Peng and Z. Liu, *Polym. Chem.*, 2014, **5**, 1573–1580.
- 9 A. Silvestre Bongiovanni, M. Molina, C. Rivarola, M. Kogan and C. Barbero, *Nanotechnology*, 2014, **25**, 495602.
- 10 J. Yang, J. Choi, D. Bang, E. Kim, E. K. Lim, H. Park, J. S. Suh, K. Lee, K. H. Yoo, E. K. Kim, Y. M. Huh and S. Haam, *Angew. Chem., Int. Ed.*, 2011, **50**, 441–444.
- 11 N. E. Monge, M. a. C. Miras and C. s. A. Barbero, *J. Comb. Chem.*, 2010, **12**, 814–817.
- 12 M. Calderón, M. A. Quadir, S. K. Sharma and R. Haag, *Adv. Mater.*, 2010, **22**, 190–218.
- 13 A. V. Kabanov and S. V. Vinogradov, *Angew. Chem., Int. Ed.*, 2009, **48**, 5418–5429.
- 14 J. C. Cuggino, C. I. Alvarez I, M. C. Strumia, P. Welker, K. Licha, D. Steinhilber, R.-C. Mutihac and M. Calderon, *Soft Matter*, 2011, **7**, 11259–11266.
- 15 M. Giulbudagian, M. Asadian-Birjand, D. Steinhilber, K. Achazi, M. Molina and M. Calderon, *Polym. Chem.*, 2014, **5**, 6909–6913.
- 16 M. Molina, M. Giulbudagian and M. Calderón, *Macromol. Chem. Phys.*, 2014, **215**, 2414–2419.
- 17 M. Bikram and J. L. West, *Expert Opin. Drug Delivery*, 2008, **5**, 1077–1091.
- 18 M. A. Molina, C. R. Rivarola, M. C. Miras, D. Lescano and C. A. Barbero, *Nanotechnology*, 2011, **22**, 245504.
- 19 T. Kawano, Y. Niidome, T. Mori, Y. Katayama and T. Niidome, *Bioconjugate Chem.*, 2009, **20**, 209–212.
- 20 M. Witting, M. Molina, K. Obst, R. Plank, K. M. Eckl, H. C. Hennies, M. Calderón, W. Frieß and S. Hedtrich, *Nanomedicine*, 2015, **11**, 1179–1187.
- 21 W. S. Huang and A. G. MacDiarmid, *Polymer*, 1993, **34**, 1833–1845.
- 22 B. Zhang, S. Sun and P. Wu, *Soft Matter*, 2013, **9**, 1678–1684.
- 23 C. S. S. R. Kumar and F. Mohammad, *Adv. Drug Delivery Rev.*, 2011, **63**, 789–808.

